Platinum Jubilee

Physical Research Laboratory
MetMeSS-2022

2nd Symposium On

“Meteoroids, Meteors and Meteorites: Messengers from Space”

24th November, Thursday

Session-II: Achondrites and Terrestrial planets: Windows to the Universe!

Session Chairs: Rajneesh Bhutani & A. Basu Sarbadhikari

Abstract #	Time	Speaker	Title of talk
Invited	15:20-15.50	J.S. Ray	Understanding Early Silicate Earth Differentiation.
S2-01	15:50-16:00	Gurpreet Kaur Bhatia	Early thermal evolution of the proto-Earth in the presence of primordial solar nebula
S2-02	16:00:16:10	Dipankar Pathak	Understanding volatile element depletion in early Solar System and the origin of volatiles in Earth using stable Sn isotope fractionation in bulk chondrites and chondrule-matrix separates
S2-03	16:10:16:20	Yash Srivastava	Understanding ancient mare volcanism from KREEP-free samples
S2-04	16:20:16:30	Anushikha Chaudhuri	Raman Spectral Characterization of Organic Matter in CI- and CM-like Clasts in a Polymict Eucrite
S2-05	16:30:16:40	Trishit Ruj	Skewed concentric crater fill deposits in the northern mid-latitudes of Mars Particulate asteroid and comet matter on the Earth.
S2-06	16:40:16:50	Alka Rani	Geological Implications of Chemical Provinces on Mars
S2-07	16:50:17:00	Sumit Pathak	Geological investigation of class-3 lunar floor-fractured crater Taruntius
S2-08	17:00:17:10	Harsh Thakur	The Lakangaon eucrite: a unique, non-cumulate piece of rock from the Vesta
S2-09	17:10:17:20	Aditya Das	Secondary minerals in Nakhlites: implication for hydration in Martian crust
S2-10	17:20:17:30	Sourajit Sahoo	Carbon isotopic variations of graphites and graphite-metal interface in Kendall County IAB iron meteorite
S2-11	17:30:17:40	Amit Basu Sarbadhikari	The Diyodar meteorite: A new fall in India

Early thermal evolution of the proto-Earth in the presence of primordial solar nebula

Gurpreet Kaur Bhatia[1]
Maharishi Markandeshwar Engineering College, Maharishi Markandeshwar (Deemed to be University), Mullana, India, 133207
gurpreetkaur@pu.ac.in

Abstract: To understand the presence of nebula volatiles in the Earth's interior, it is essential to study the early thermal history of proto-Earth (the main accretion phase of Earth) during the lifetime of the solar nebula. Recent studied have also suggested that the main accretion phase of Earth accreted and differentiated rapidly within the initial ~5 Ma of the formation of the solar system [1]. The early accreted proto-Earth could have significantly captured primordial nebula gas due to its gravity. We performed numerical simulations to study the early thermal evolution and core-mantle segregation of the proto-Earth by considering the decay energy of short-lived radionuclide (SLR) ^{26}Al and blanketing effect of the captured proto-atmosphere of solar composition during accretion [2]. The results of this study suggest significant melting of proto-Earth's interior due to SLR ^{26}Al. The blanketing effect of the captured primordial atmosphere melted the surface silicates to form magma ocean at the surface during the final stages of accretion. The nebula volatiles could dissolve into the magma ocean due to dissolution and could partition into the interior of early Earth [3-4]. The outcomes of present work could have implications to explain the presence of nebula volatiles in the interior and timescale of formation of atmosphere on the early Earth.

References: [1] Schiller, M., Bizzarro, M., Siebert, J., 2020. Sci. Adv. 6 (7), eaay7604. [2] Bhatia 2022. Under Review. [3] Sharp, Z.D., 2017. Chem. Geol. 448, 137–150. [4] Williams, C.D., Mukhopadhyay, S., 2019. Nature 565, 78.

Understanding volatile element depletion in early Solar System and the origin of volatiles in Earth using stable Sn isotope fractionation in bulk chondrites and chondrule-matrix separates

Dipankar Pathak[1,*], Yogita Kadlag[2], Klaus Mezger[1], Gopalan Srinivasan[3]
[1]Institut für Geologie, Universität Bern, Baltzerstrasse 1+3, CH 3012, Bern, Switzerland
[2]Physical Research Laboratory, Ahmedabad, Gujarat, India
[3]Society for Research in Space Science & Earth Habitability**, Bhopal 462016, Madhya Pradesh, India. *Corresponding author email: dipankar.pathak@geo.unibe.ch
(**Registration under process)

Introduction: The ability of a planet to host life is determined by several factors during their formation and further evolution (e.g. geochemical differentiation, tectonic activities). The presence of volatiles compounds (such as H_2O, CH_4, CO_2, O_2 etc.) are also crucial in building the suitable environment for life to sustain and evolve over time. Hence, understanding the origin of volatiles (especially H_2O) in rocky planets like Venus, Earth, and Mars is a challenging problem to assess similar habitable condition of life in other similar extraterrestrial bodies. However, H_2O being quite volatile, the original isotope signatures of H and O in the various solar system materials are modified from the nebular state, making it very difficult to interpret the measured isotope ratios in these materials, with reasonable uncertainties. This problem can be circumvented by using the isotopes of other volatile elements as proxies, to gain information about the physico-chemical conditions which causes their fractionation in the solar nebula. Tin, which is a moderately volatile element (50% condensation temperature of 704 K) [1], with ten naturally occurring stable isotopes, can serve as such a suitable proxy. Apart from showing strong depletion in most planetary materials, Sn also shows chalcophile/siderophile properties. This makes it a valuable proxy to also extract information about planetary core formation, in addition to understanding the origin of volatiles in rocky planets.

Methodology: In this work, we present a wet chemistry based method to determine the mass dependent isotope fractionation of Sn in various chondritic meteorites and terrestrial rocks, using double spike MC-ICP-MS measurements. A total of 14 terrestrial rock reference standards and 37 bulk chondritic meteorites, as well as the matrix and chondrule separates of some of these chondrites, were processed using table-top hotplate based acid dissolution, followed by a two-stage column chromatography, to isolate Sn from several isobarically interfering as well as major matrix elements [2].

Results and Discussion: The measured $\delta^{122/118}$Sn showed the largest variations (i.e. difference between the most and least fractionated sample) in bulk ordinary chondrite (OC) (1.3 ‰; n = 12), along with a large scatter, which is consistent with previous studies ($\delta^{122/118}$Sn = -1.08 to 0.543 ‰ [3], $\delta^{124/118}$Sn = -2.02 to 0.64 ‰ [4]). Such randomly scattered δ^{122}Sn can be attributed to parent body metamorphism or impact induced fractionation as observed in case of tektites [5]. This range in variations of $\delta^{122/118}$Sn is intermediate in carbonaceous chondrites (CC) (0.54 ‰; n = 15) and the least in enstatite chondrites (EC) (0.24 ‰; n = 9). In terms of overall Sn abundance, the bulk OCs tend to be the most depleted ([Mean Sn ± 2sd] = 0.33 ± 0.13 μg/g), with CCs having an intermediate ([Mean Sn ± 2sd] = 0.77 ± 0.59 μg/g), and ECs showing the least depletion ([Mean Sn ± 2sd] = 1.77 ± 0.59 μg/g) of all. The measured $\delta^{122/118}$Sn of OCs, CCs and ECs also spreads across the range of a presently estimated bulk silicate Earth (BSE) composition using Komatiites ($\delta^{122/118}$Sn = 0.49 ± 0.11 ‰ 2sd) [6]. A systematic variation in $\delta^{122/118}$Sn relative to $[Sn]^{-1}$ is also observed within the CC group, highlighting the role of volatility during condensation in the nebular disk. The pooled Allende chondrules shows a distinct $\delta^{122/118}$Sn than the matrix.

References: [1] Lodders K. (2003) *The Astrophysical Journal of Geophysical Research* 591(2), 1220. [2] Pathak D. et al., (2022) In preparation. [3] Creech J.B. & Moynier F. (2019) *Chemical* Geology 511, 81-90. [4] Wang X. et al. (2021) *Geochimica et Cosmochimica Acta* 312, 139-157. [5] Creech J.B. et al. (2019) *Chemical Geology* 528, 119279. [6] Badullovich N. et al. (2017) *Geochemical. Perspective Letters*, 5, 24-28.

Understanding ancient mare volcanism from KREEP-free samples

Yash Srivastava[1,2,*], Alka Rani[1,2], Varsha M Nair[1,2] and Amit Basu Sarbadhikari[1]
[1]Physical Research Laboratory, Ahmedabad 380009, India
[2]Indian Institute of Technology Gandhinagar, Gujarat 382355, India,
*E-mail: yash@prl.res.in

Apollo, Luna, and recent Chang'E 5 sample collection missions have provided invaluable understanding of the chemical and thermal evolution of the Moon. The lunar basalts sampled by these missions are the major source of information about the lunar interior evolution after the major differentiation process [1]. Typically understood, lunar basalts are formed by partially melting of the mantle, with heating assisted by the mixing of heat-producing incompatible element-rich layers known as "KREEP" [2]. And it was believed that the high abundance of incompatible trace elements measured in these samples is the tell-tale of the lunar mantle overturn process where KREEP mixes into the source of mare basalts. However, an alternate hypothesis posits that some lunar basalts might have a KREEP-free origin where ITE enrichment is produced purely through simple magmatic processes such as low-degree melting followed by extensive fractional crystallization [3,4,5].

In this work, we perform detailed petrological and geochemical investigation of lunar basaltic meteorite Asuka-881757 along with other KREEP-free samples to understand the early thermo-chemical evolution of the Moon. Our major and trace element modelling shows that these basalts were derived from low-degree partial melting of pyroxene rich mantle. The applied thermodynamic modelling further suggests these KREEP-free basalts were sourced from a relatively cool and shallow pyroxene-rich mantle distinct from later-erupted (<3.8 Ga) KREEP-bearing basalts, indicating a fundamental change in melting regimes in the Moon.

References: [1] Shearer, C.K., et al., (2006) *Rev. Mineral Geochem*, ***60*****(1)**, pp.365-518. [2] Neal, C.R. and Taylor, L.A., (1992). *GCA*, ***56*****(6)**, pp.2177-2211. [3] Borg, L.E., et al., (2009) *GCA*, ***73*****(13)**, pp.3963-3980. [4] Elardo, S.M., et al., (2014) *MAPS*, ***49*****(2)**, pp.261-291. [5] Tian, H.C., et al., (2021) *Nature*, ***600*****(7887)**, pp.59-63.

Raman Spectral Characterization of Organic Matter in CI- and CM-like Clasts in a Polymict Eucrite

Anushikha Chaudhuri[1*], Subhasmita Swain[2], Swarna Prava Das[2],
Markus Patzek[3], S.S Rout[2]
[1]Department of Physical Sciences, Shiv Nadar University, Greater Noida, Uttar Pradesh 201314
[2]SEPS, National Institute of Science Education and Research (NISER) Bhubaneswar, Khorda, Jatni, Odisha 752050
[3]Institute for Planetology, University of Muenster, Wilhelm-Klemm-Str.10, 48149 Muenster, Germany
*Corresponding author. E-mail: anushikhac@gmail.com

Introduction:

Meteoritic breccias are of vital importance for knowing the dynamics and collisional evolution of meteorite parent bodies [1]. Many of these brecciated meteorites contain xenolithic clasts which are fragments of different types of meteorites. Some of these clasts can represent materials which are not present in our collection of meteorites and therefore have valuable potential for further research. In our study, we investigate the Raman spectral characteristics of the embedded organic matter in CI/CM-like clasts in a brecciated polymict Eucrite. Study of CI/CM-like clasts in polymict ureilites and HEDs show that they are added to the surface of the parent asteroid as micrometeorites or low velocity impactors. The purpose of our study is to gain better understanding of the properties of organic matter in CI/CM-like clasts in a polymict Eucrite and then compare them to micrometeorites.

Samples and Methods:

Raman spectroscopy is a non-destructive technique that is sensitive to the structural order of organics. Here, we studied a polymict Eucrite of NWA752 (PL14058-A) having 9 clasts. We have used HORIBA LabSpec 6 Raman spectrometer. Over 100 Raman Spectra were acquired from 2 different clasts – Clast 10 and Clast A1. The spectral signature has been obtained with grating of 600 lines/mm, with an acquisition time of 20-40 seconds and with beam energy of <1mW. From the spectra, a linear background from 1000-1800 cm^{-1} has been subtracted. Fitting of the peaks has been done using Lorentzian function for G band and BWF for D band, with coefficient of determination (R^2) above 0.9.

Result:

Sample observed shows that Clast 10 and Clast A1 is of the type CM-like and CI-like respectively. In both cases, Raman spectra shows two peaks (D and G band). The $FWHM_D$ for Clast 10 and Clast A1 is in the range of 116-283.51 cm^{-1} and 260.489-100.306 cm^{-1} respectively. The peak positions of Clast A1 and Clast 10 for bands (D, G) shows Raman shifts of (1375.28 cm^{-1}, 1557.94 cm^{-1}) and (1366.62 cm^{-1}, 1573.251 cm^{-1}) respectively. Figure 1 shows that the organic matter in Clast A1 plots in the range of Ultracarbonaceous Antarctic Micrometeorites (UCAMM) and fine-grained hydrated micrometeorites and Clast 10 plots in the region of fine-grained hydrated micrometeorites [2].

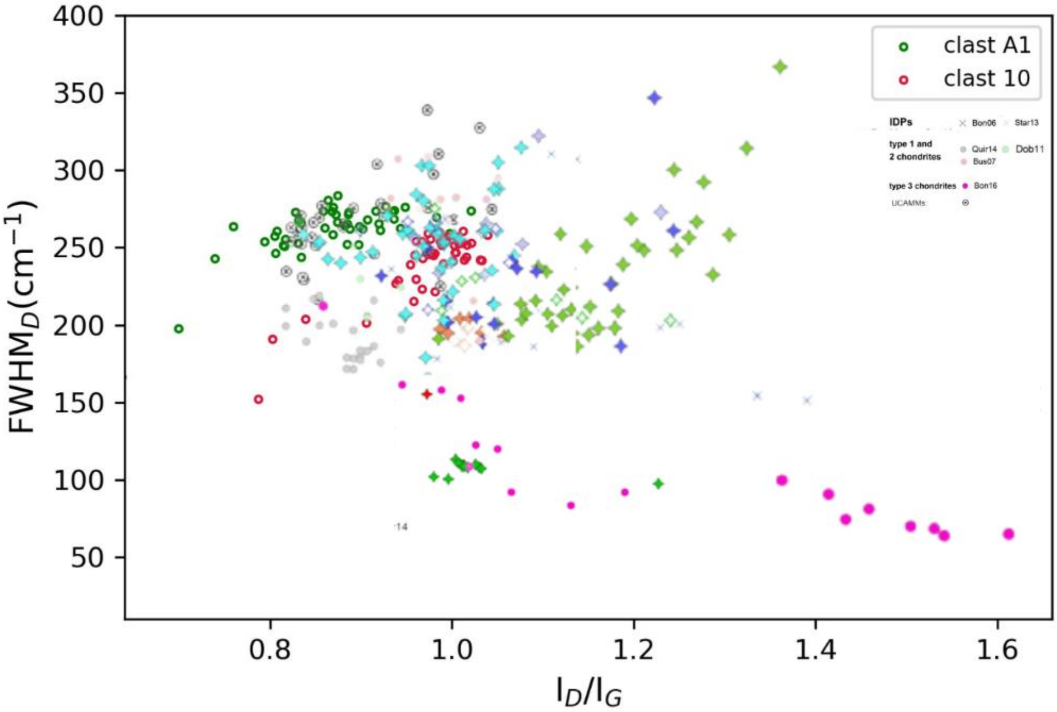

Figure 1: FWHM Vs. Intensity Ratio plots for various meteorite samples. Image source [2].

Conclusion and Future Work:

From the preliminary study of our sample, we observe that the organic matter in the CI-like clasts and CM-like clasts is similar to Ultracarbonaceous Antarctic Micrometeorites (UCAMMs) and hydrated fine-grained micrometeorites respectively [3]. Further research involves Raman spectral characterization, mineralogical studies and classifications of all the clasts in our samples using Scanning Electron Microscope (SEM) and Transmission Electron Microscope (TEM).

References:

[1] Bischoff A., Scott E. R. D., Metzler K., and Goodrich C. A. (2006). The University of Arizona Press. 679–712.
[2] Battandier M. et al., (2018). *Icarus*, 306:74-93
[3] Patzek M. et al. (2018). *Meteoritics & Planetary Science*, 1-22.
[4] Gounelle M., Zolensky M. E., Liou J.-C., Bland P. A., and Alard O. (2003). *Geochimica et Cosmochimica Acta*. 67:507–527.

Skewed concentric crater fill deposits in the northern mid-latitudes of Mars

Trishit Ruj[1, *], Hanaya Okuda[2], Tomohiro Usui[1], Goro Komatsu[3]
[1] Institute of Space and Astronautical Science (ISAS), Japan Aerospace Exploration Agency (JAXA), 3-1-1 Yoshinodai, Sagamihara, Kanagawa 252–5210, Japan.
[2] Department of Ocean Floor Geoscience, Atmosphere and Ocean Research Institute, University of Tokyo, Kashiwanoha 5-1-5, Kashiwa, Chiba 277-8564, Japan.
[3]International Research School of Planetary Sciences, Università d'Annunzio, Viale Pindaro 42, 65127, Pescara, Italy

*Corresponding author E-mail: trishitruj@gmail.com

Introduction: Mid-latitudes of Mars preserve geomorphological signatures that indicate the presence of volatile-rich zones as a possible reservoir for water ice at an accessible subsurface depth [1, 2, 3]. Present day, surface water ice is concentrated in the polar regions, however, in past, with increasing obliquity, with the increase in the surface solar insolation and atmospheric CO_2, ice accumulation of ice shifted towards the low to mid-latitudes [4, 5, 6]. Episodic change in the obliquity also resulted in lobate debris aprons LDA, concentric crater fill (CCF), and lineated valley fill (LVF) like landforms there in the mid-latitudes [3]. Morphologically, these landforms resemble terrestrial glacial geological features formed by viscous deformation due to the flow of rock and ice [2, 7]. Exploration of these glacial deposits could potentially help in finding near-surface deposits during future explorations.

Here, we focused on the craters (25ºN–40ºN latitudes) of the Arabia Terra region, of diameters >2 km. In general, CCF deposits are Amazonian-aged (~60–300 Ma) glacial landforms [2, 8, 9] and multiple hypotheses have been proposed to explain the origin of these deposits and they include "ice-enhanced regolith creep" [10], debris derived from bedrock recession along scarps due to sublimation of ground ice or the emergence of groundwater [11], mobilization and seasonal flow of talus by diffusional emplaced pore ice [9], and debris-covered glacier [2, 12].

In this research, we did a geomorphological investigation using the Thermal Emission Imaging System (THEMIS)–InfraRed (IR) daytime [13] coupled with a high-resolution Stereo Camera (HRSC)-MOLA blended Digital Terrain Models (DEM) (200 m/pixel) [14], Context (CTX) camera (6 m/pixel) [15] and a High-Resolution Imaging Science Experiment (HiRISE) [16] in ArcGIS platform. For the solar radiation model, we have computed the daily mean solar insolation for a model crater at 30ºN latitude [16].

Results: Our preliminary observation suggests that a handful number of craters in the study area latitude have CCF deposits on their floors (Figure 1). High-resolution images reveal that CCF deposits on average are wider at the southwestern part of the crater floor.

Therefore, tried to address the question 'how has the annual temperature contributed to the ice deposits in the southwest part of the crater?' and 'why are the deposits concentrated on the southern inner wall of the crater?'

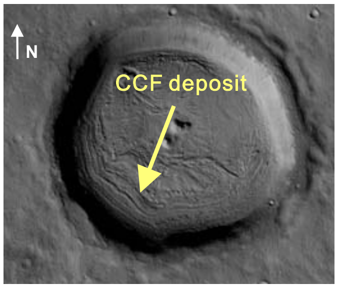

Figure 1: The low-intensity deposit concentrates only on the southwestern sector of the crater floor. The deposit is concentrated on the southwest part of the floor.

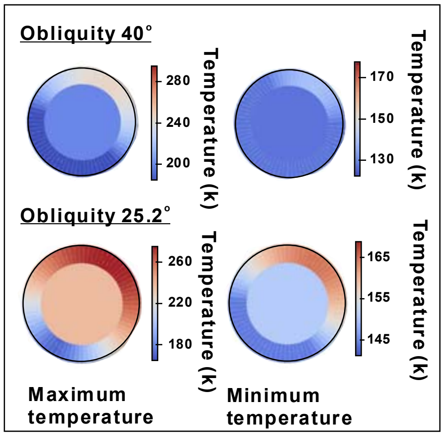

Figure 2: Variation of average maximum and minimum temperature in the crater wall. This result coincides with the observation data from the Arabia Terra region.

Discussion and Conclusion: The parallel ridge and trough topography is developed within the southwestern part of the craters in most cases. This apparent trend in the deposition pattern could also be correlated with the hypothesis that ice on the southern part is preferentially melted whereas in the northern part it is mostly sublimated [8]. 1D radiative-convective model (derived from a full 3D GCM) suggests that the southwestern part (Figure 2) of the crater walls remains coldest throughout the year. Therefore, the southwestern part of the craters became cold traps for the ice to accumulate, and when the temperature rose, it melted and formed parallel ridge and floor topography following the curvature of the inner crater wall.

Future work could consist of using a surface temperature model as opposed to a direct insolation one to explain the observed south-southwest trend.

References: [1] Levy, J. S. et al. (2021) Proc. Natl. Acad. Sci. U. S. A. 118, 1–7. [2] Levy, J. S. et al. (2010) Icarus 209, 390–404. [3] Berman, D. C. et al. (2009) Icarus 200, 77–95. [4] Head, J. W. et al. (2003) Nature 426, 797–802. [5] Forget, F. et al. (2006) Science (80). 311, 368–371. [6] Levrard, B. et al. (2004) Nature 431, 1072–1075. [7] Mangold, N. (2003) JGR-Planets 108, 8021. [8] Berman, D. C. et al. (2005) Icarus 178, 465–486. [9] Squyres, S. W. (1979) JGR-Solid Earth 84, 8087–8096. [10] Zimbelman, J. R., and Clifford, S. M. (1989) 19th LPSC, 397–4-7. [11] Sharp, R. P. (1973) JGR. 78, 4073–4083. [12] Levy, J. S., et al. (2009) Icarus 202, 462–476. [13] Christensen, P. R. et al. (2004) Space Sci. Rev. 110, 85–130. [14] Fergason et al., (2018) Astrogeology PDS Annex, US Geological Survey. [15] Malin, M. C. et al. (2007) JGR 112, E05S04. [16] McEwen, A. S. et al. (2007) JGR Planets 112, 5–7.

S2-06

Geological Implications of Chemical Provinces on Mars

Alka Rani*,1, Yash Srivastava1,2, Varsha M. Nair1,2, and Amit Basu Sarbadhikari1

1Physical Research Laboratory, Ahmedabad, India, 2Indian Institute of Technology, Gandhinagar, India, *Email: alka@prl.res.in

We consolidate the three semi-independent GIS-based chemical province delineating methods using Mars Odyssey Gamma and neutron spectroscopy (GRS) based on latest geochemical maps to demarcate the chemical provinces on Mars and interpret new provinces that are revealed. Earlier studies used individual techniques with limited chemical data, resulting in poor sensitivity in highlighting the chemical provinces [1-3]. Furthermore, due to unavailability of Sulfur data, important information regarding volatiles was missing. Our study sheds light on the major geological processes responsible for the formation of chemically distinct provinces. Three provinces are explored in detail: Lunae Planum (depleted in K, Th, and H_2O), Medusae Fossae (volatiles enriched: Cl, S, H_2O with Fe), and Acidalia Planitia (enriched in K, Th with Al depletion), to characterize possible flood basalt events that straddle the deepest strata of Mariner Valley, to determine the source of possible global ashfall units, and to consider the relative roles of igneous versus aqueous environments in a major transition zone from highlands to lowlands of Mars. Initial results indicate that the depletion of K and Th in Lunae Planum is substantially aligned with other Hesperian-aged volcanic regions, particularly the nearby Thaumasia Planum volcanic province. The volatile enrichment in Medusae Fossae region shows evidence of resulting from volcanic emissions as large pyroclastic deposits. Whereas, enrichment of absolute abundances of K and Th with Al depletion in Acidalia Planitia region is more representative of variations in melt generation with a low aqueous alteration process.

Refernces: [1] Karunatillake et al., (2009), *JGR, 114*. [2] Taylor et al., (2010), *Geology, 38,* 183-186. [3] Gasnault et al., (2010), *Icarus*, 226-247.

Geological investigation of class-3 lunar floor-fractured crater Taruntius

Sumit Pathak*, Himela Moitra, and Saibal Gupta
Department of Geology & Geophysics, Indian Institute of Technology, Kharagpur, India
*Corresponding author E-mail: spathak.sac@gmail.com

Introduction: Recently, lunar floor-fractured craters (FFCs) have emerged as an important research topic in order to comprehend and unravel the various morphological and mineralogical entities that have implications for the magmatic and thermal evolution of the lunar surface throughout its geological history. [1-8]. We have used multiple datasets from different lunar missions to examine the geology of class 3 FFC Taruntius in this study. Crater Taruntius is an excellent example of a class-3 FFC. This crater is located on the northwestern edge (5.6°N, 46.5°E) of the Mare Fecunditatis, separating it from Mare Tranquillitatis. It is a nearly circular-shaped Copernican crater with a diameter of ~ 58 km. This crater features a notable central peak area as well as some concentric fractures in the crater floor. A dark spot has been identified on the SW corner of the central peak region.

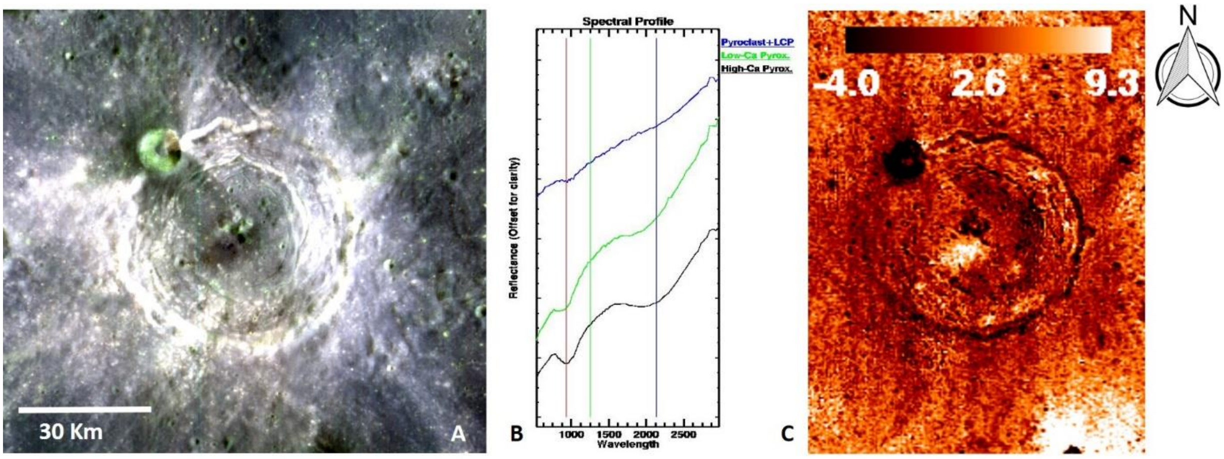

Figure 1: (A) FCC mosaic of crater Taruntius from M^3 datasets. (B) Representative reflectance spectra of various minerals derived from FCC mosaic. (C) TiO_2 abundance map of crater Taruntius.

Dataset and Methodology: In this study, we have analyzed the mineralogical variability with respect to the morphology of the crater. For mineralogical analysis, the photometrically and thermally corrected level-2 hyperspectral datasets of Moon Mineralogy Mapper (M^3) onboard Chandrayaan-1 have been used [9, 10]. The WAC-TiO_2 global data (Table 1) given by [11] have also been used to estimate the TiO_2 abundance over the studied site. To study the morphological features, the global datasets with 100-m spatial resolution from the Wide-Angle Camera of NASA's Lunar Reconnaissance Orbiter (LROC-WAC) have been used [12] along with the Lunar Orbiter Laser Altimeter-Digital Elevation Model (LOLA-DEM) datasets with the 30-m spatial resolution for the topographic study of the crater [13, 14]. To understand the mineralogical variation in the studied region, a false color composite (FCC) mosaic (Fig. 1) has been prepared by assigning the 930-nm, 1249-nm, and 2137-nm spectral bands of M^3 strips in the red, green, and blue channels, respectively. Subsequently, we obtained the reflectance spectra from this FCC image to distinguish various mineralogical constituents (Fig. 2).

Results and Discussions: The representative reflectance spectra of the study area were analyzed for the detection of major mineral phases, based on the diagnostic absorption features of the chief mafic minerals. In Figure 1, a few patches of the mafic exposures in the shades of yellow and green are present along the central peak area and the crater floor. The spectra extraction locations are marked by the polygons. The major mafic mineralogies are represented by Low-Ca pyroxenes (LCPs) and High-Ca pyroxenes (HCPs) and are characterized on the basis of their double absorption features near 935-nm with 1985-nm, and 985-nm with 2165-nm respectively (Fig. 1B). The central peak area is mainly composed of LCP (Fig. 1B). Most of the spectral signatures of HCP (Fig. 1B) could be observed in and around the central peak region. Similarly, the reflectance spectra of these pyroxene mineralogies could be identified from the fresh craters from various parts of the crater floor, which might have re-excavated from the underlying pyroxene-plagioclase-rich mineralogy to the surface. Some mounds composed of LCP-bearing mineralogies have been found along both sides of the fracture placed towards the northwest side of the central peak area. These LCPs might be crystallized from the melt that escaped through those fractures during the time of post-impact modifications. Some nearly featureless spectra were also found which have very low reflectance values with minute absorptions in 1000 and 2000 nm, which could be represented by the occurrence of pyroclast-bearing units in the region. Hence, the mineralogical analysis results help us to comprehend that the central peak region is enriched in deeper crustal mafic mineral assemblages, which were excavated due to the impact event and the subsequent magmatic event which modified the mineralogy on the floor. Additionally, the TiO_2 abundance map suggests that the pyroclastic patch near the southern portion of the central peak has a high abundance of TiO_2 (Fig. 1C). In case of morphological analysis, the LROC-WAC image shows the concentric fracture system around the central peak region and adjacent to the periphery of the crater floor and wall terraces along the inner flank of the crater rim (Fig. 2). Some fractures were generated during the later phase of ductile deformation and cross-cut the earlier ones. The topography of the crater floor suggests that the peripheral region of the floor is undulated and tormented (Fig. 2). From the spatial profiles (Figs. 2A and 2B) derived from LOLA-DEM data, we can identify the well-defined moat region adjacent to the crater wall region. The spatial profiles also indicate that the crater floor is uplifted on the central portion with various types of concentric fractures around it.

Conclusion: From the present study it is concluded that the crater Taruntius is characterized by a nearly rounded periphery, uplifted deformed crater floor, concentric fractures, and pronounced moat regions belonging to typical characteristics of Class-3 lunar FFC [1, 2]. The composition and mineralogy identified through the M^3 datasets indicate the presence of mafic minerals, namely, Low-Ca pyroxenes and High-Ca pyroxenes, which might be excavated to the surface from an underlying mafic plutonic body during the crater-forming impact event. Additionally, the morphology of the crater floor and the results of the mineralogical analysis also show evidence of late-stage pyroclastic activity along with the significant abundance of TiO_2-bearing deposits in the area. Further detailed studies are envisaged for the deeper crustal significance and understanding of the litho-evolutionary mechanisms of the FFC.

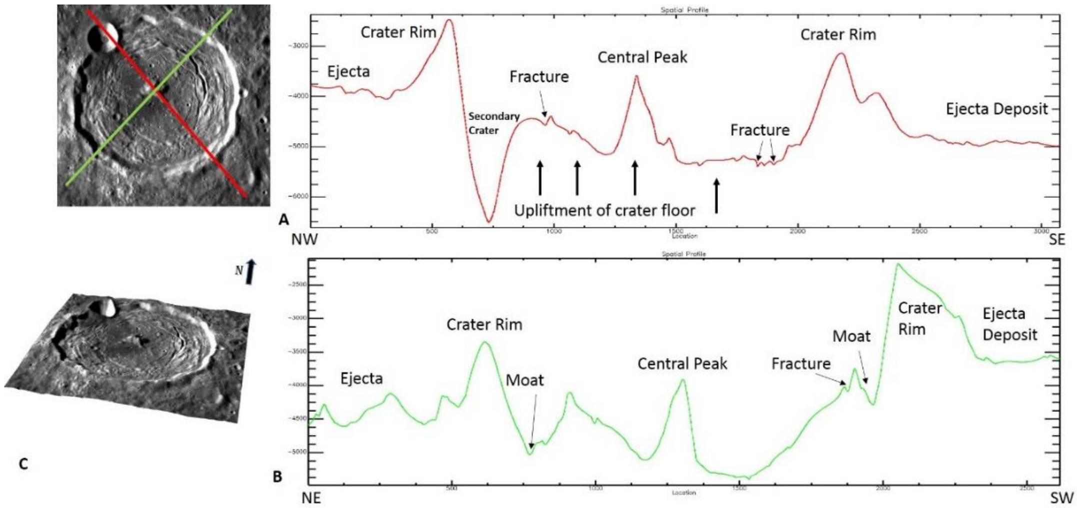

Figure 2: The figures show the (a) NW-SE (in red) and (b) NE-SW (in green) spatial profiles of crater Taruntius derived from LOLA-DEM data, which show various morphological units over the crater floor. (c) The 3D image of crater Taruntius has been prepared for topographic analysis.

References: [1] Jozwiak et al. 2012, JGR, Vol. 117, E11005. [2] Jozwiak et al. 2015, ICARUS 248, 424-447. [3] Bennett et al. 2016, Icarus, 273, 296-314. [4] Martinot et al., JGR, doi:10.1002/2017JE005435. [5] Pathak et al. 2015, EPSC, Vol. 10, EPSC2015-550. [6] Pathak et al. 2018, LPSC, XXXXIX, 2046. [7] Pathak et al. 2021, ICARUS, 360, 114374. [8] Schultz 1976, The Moon, Vol. 15, 241-273. [9] Goswami and Annadurai, 2009; Curr. Sci., 96(4), 486-961. [10] Green et al. 2011, JGR, Vol. 116, E00G19. [11] Sato et al. 2017, ICARUS, 296, 216-238. [12] Boardman J. et al. (2011) JGR 116, E00G14. [13] Robinson et al. 2010, 38th COSPAR Scientific Assembly, 15–18 July 2010. Bremen, Germany, 11. [14] Smith et al. 2010, GRL, 37(18).

The Lakangaon eucrite: a unique, non-cumulate piece of rock from the Vesta

Harsh Thakur[1,*], Dwijesh Ray[2] and Sambhunath Ghosh[3]
[1]Centre for Earth Sciences, Indian Institute of Science, Bangalore
[2]Planetary Sciences Division, Physical Research Laboratory, Ahmedabad
[3]54/3 Mahendra Banerjee Road, Kolkata, 700 060, India
*harshthakur@iisc.ac.in

Introduction: The HED (Howardite, Eucrite, Diogenite) meteorites are thought to have originated from a common differentiated parent body Asteroid 4-Vesta. The 4-Vesta represents one of the largest celestial bodies in the main asteroid belt and suggested the earliest stages of basaltic volcanism in the Solar System. The genetic link of the HED meteorite clan with asteroid 4-Vesta was established based on the similarity of petrological and spectral characteristics and the Vesta-HED connection was further consolidated by the recent Dawn mission. The eucrite is known for its typical basaltic texture similar to the terrestrial basalts. The Lakangaon eucrite fell on Nov 14, 1910, in the Nimar region of British India, near present-day Khandwa district, Madhya Pradesh, India, and is one of 261 approved meteorites classified as Eucrite-monomict as of date (Met. Bulletin). Lakangaon is a lesser-known eucrite as compared to other known Indian eucrites; hence it has not drawn much attention. Lakangaon was deemed the most Fe-rich eucrite [1], perhaps because it crystallised later than most Eucrites. Though the Lakangaon was described as Fe-rich eucrite in literature, detailed petrography and mineral chemistry were never discussed and explored in detail. Integrated mineral phase and whole-rock chemistry are always key in order to understand magmatic crystallisation event, identification of igneous processes of parent body and to constrain the thermal and chemical evolution of 4 Vesta. Hence, we discuss some new findings of petrochemistry of Lakangaon eucrite.

Methodology: This study was carried out using two polished thick sections of the Lakangaon sample. All petrographic characterisation, textural observation, BSE imaging, and data collection were performed using an FE-EPMA (model JEOL 8530F, Japan) equipped with EDS and five WDS. The minerals were analysed, and the images were taken using a typical accelerating voltage of 15keV and 15 nA sample current and beam size of 1µm. Natural and synthetic mineral standards were used for calibration. The peak counting time of the majority of elements was kept at 10s with the background of 5s (except for Na and K, it was 7s). The whole-rock trace element analyses were determined using a Q-ICPMS by ThermoFisher. BHVO2 was used for calibration. The accuracy of the analyses is better than 10%.

Mineral chemistry and whole-rock chemistry: Lakangaon, a brecciated basaltic eucrite, is dominated by mafic pyroxene and felsic plagioclase grains. Other accessory minerals include quartz, ilmenite, chromite, and troilite. The overall mineral modes of the sample include 36% pyroxene, 59.4% plagioclase + silica, and the accessory minerals like ilmenite, Mg-Al chromite, and troilite make up 0.9%. The pyroxenes composition ranges from ferrosilite to pigeonite to augite. The compositional trend of pyroxene is linear. Pigeonite primarily occurs as exsolution lamellae within the ferrosilite as well as in augite. Takeda and Graham [2] defined six types of eucrites, where type 1 is a pristine basalt which has suffered very limited subsequent metamorphism, while type 6 has been reheated and extensively metamorphosed. According to this analysis, Lakangaon falls in type 5 eucrite. The type 5 eucrites contain exsolved pigeonites with homogeneous host composition.

Troilite was pure FeS, with Cr, Co and, Ni below the detection limit. For plagioclase, only pyroxenes have been detected to be small inclusions. Clouding in pyroxene and plagioclase has been interpreted to be the result of the exsolution of minor components which became incompatible and crystallised on microfractures and other nucleation sites during post-brecciation metamorphism. The phases found in clouding form when silicate FeO reduces to metallic Fe in both pyroxene and plagioclase and possible redox of Cr^{+2} to Cr^{+3} in pyroxene) [3]. Plagioclase occurs as separate aggregates as well as plagioclase laths in pyroxenes in Lakangaon. The range is $An_{88.47-89.99}$ which refers to bytownite-anorthitic composition. Silica composition is almost pure silica. Ilmenite is present as relatively large inclusions in pyroxenes as well as plagioclase, sometimes also in association with silica, in various shapes and sizes (8µm to 150µm), from subhedral to euhedral to wide elongated (bottle-like) shape. Chromite occurs in Lakangaon as both inclusions in pyroxenes, plagioclase and also in silica. It is relatively smaller in size as compared to ilmenite, mostly anhedral, and most grains are of the size 2µm to 10µm, with some grains up to 75µm in association with ilmenite. Troilite occurs as very fine inclusions in pyroxenes and causes clouding. Also, it is pure FeS with Co, Cr, and Ni below detection limits. It is mostly rod and bleb shaped when occurring in clouding (<0.5 µm), and when it exists as a grain, it is mostly anhedral, and size is <10µm. A few grains of zircon were also identified in this study. All of them were either associated with ilmenite or as isolated grains. The zircon grains in Lakangaon are generally less than 10µm in size. The rare-earth element (REE) pattern of Lakangaon is almost flat (La/Yb_N: 0.70), while the slope of LREE and HREE vary from 0.92 to 0.76, respectively. This sample shows a depleted pattern of REEs as compared to the literature data. This can be attributed to sampling bias. The literature values show a negative Eu anomaly, whereas the data from this study does not show any anomaly.

Discussion: Lakangaon is a basaltic eucrite which falls into the Nuevo Laredo group, as revealed by the chemistry of pyroxenes and the bulk rock chemistry. The pyroxenes, particularly pigeonite, are exsolved in augite and ferrosilite. It must have been rapid cooling which preserved this variation of pyroxenes [4]. Troilite, metal, and silica inclusions could have been caused by a reducing agent operating on typical basaltic eucrite pyroxene compositions. A probable reducing agent is sulphur vapour. Most basaltic eucrites may have undergone secondary subsolidus reheating processes [3]. Zircons from metamorphosed eucrites may have undergone solid-state recrystallisation during subsolidus reheating events [5]. Zircons from basaltic eucrites must have originated in melts that were saturated in Zr and Si. These melts can occur as a result of the crystallisation of constituent minerals like clinopyroxene and plagioclase [6].

Clouding preserves and reflects a portion of the history of minerals post-crystallisation. A thorough investigation should improve understanding and interpretation of the last stage of planetary processing in the parent body(ies) of eucrites. Future studies are aimed to address the following questions: (1) The majority of clasts of Lakangaon appear as cumulate texture with anomalous Ti, Fe and Cr abundance suggesting for an anomalous eucrite? (2) Is the Fe-rich pyroxene resulted due to advanced crystal fractionation effect, or some other processes are also involved to explain the anomalous geochemical characters? (3) U-Pb geochronology will help not only to date the magmatic crystallisation event but also the duration of magmatism of parent body vesta and to constrain the thermal and chemical evolution of 4 Vesta. The older ages of zircon often imply early asteroidal collisions and help in finding the linkages for evidence of LHB, (4) Whether Lakangaon represents a residual melt of magma ocean or a primary partial melt and finally (5) Do all the eucrites share a common parent body origin or have a distinct parent asteroid?

References: [1] Warren P. H. et al. (1985). *Meteoritics, 20*, 779. [2] Takeda, H., & Graham, A. L. (1991). *Meteoritics, 26*(2), 129-134. [3] Harlow, G. E., & Klimentidis, R. (1980). *LPSC Proceedings* (Vol. 11, pp. 1131-1143). [4] Yamaguchi A. et al. (2001) *GCA, 65*(20), 3577-3599. [5] Hoskin, P. W. O., & Black, L. P. (2000). *JMG, 18*(4), 423-439. [6] Haba, M. K et al. (2014). *EPSC, 387*, 10-21.

Secondary minerals in Nakhlites: implication for hydration in Martian crust

Aditya Das[1,3*], Alik S. Majumdar[2], Dwijesh Ray[1]

[1]Planetary Science Division, Physical Research Laboratory, Ahmedabad, Gujarat 380009
[2]Department of Applied Geology, Indian Institute of Technology (Indian School of Mines) Dhanbad
[3]Indian Institute of Technology Gandhinagar, Gujarat 382355

*Corresponding Author E-mail: [1]adityda s@prl.res.in

The presence of hydrated, secondary minerals on Mars suggests that it was relatively warm and wet in its early Noachian days [1]. The phyllosilicate-bearing deposits on Mars not only provide an essential constraint on the early water environment but also are known as preferred landing sites for the past, ongoing, and future Mars rover missions for their unique potential for preserving the biosignatures. The majority of secondary minerals from the Noachian era on Mars include Fe-Mg phyllosilicate [2] and occur mainly at the central peak of a large, complex crater. In contrast, the secondary minerals in Martian meteorites are generally recognized as iddingsite, saponite, serpentine, and jarosite [3] in the Nakhlites meteorites. So far, eight nakhlites have been identified, and the majority of them are found in hot and cold deserts. The nakhlites are known for basaltic cumulate clinopyroxene (often olivine bearing) and are thought to be formed from thick lava flow or shallow sill [4,5]. The ubiquitous presence of secondary minerals in nakhlites provides unique and important insights into water-rock interaction on Mars. In this study, we discuss the microtextural characteristics and mineral chemistry of secondary minerals.

The iddingsite generally occur as fracture-filling within the olivine grains [6]. The mesostasis is comprised of extremely fine-grained materials and clinopyroxenes are comparatively less altered than that of olivine. Under plane polarized transmitted light, iddingsite appears as light brown. Under Back Scattered Electron (BSE) image, the veins of the iddingsite appear as often protruding inwards from the grain margin or often crosscut the whole olivine grains. In higher magnification, serrated structures of iddingsite veins are also noticed. In the SiO_2-MgO-$FeO_{(T)}$ ternary diagram the Martian iddingsite falls along the SiO_2-FeO line with increasing enrichment of SiO_2 that shows a characteristic deviation in composition as compared to its terrestrial counterpart. The overall Al depletion and chemical composition resemble the poorly crystalline phases. However, a few compositions are apparently similar to laihunite.

The poorly crystalline nature of the majority of iddingsite is consistent with rapid chilling and emplaced near the surface. The fractures formed in olivine due to deformation are not magmatic but rather resulted due to post magmatic, impact-induced processes. The impact was relatively weaker in nature and distinct from the nakhlite magmatism event and ejection impact. The non-crystalline behavior of iddingsite also supports its formation is unlikely and for a part of larger convection of hydrothermal alteration rather suggesting short-lived and limited water conditions either at a margin of a large crater or formed at a simple crater. The greater magnitude of alteration of olivine as compared to pyroxene suggested for considerably higher reactivity of olivine in presence of Martian fluids under oxidizing [7], intermediate temperatures, low water-rock ratio environment.

References: References: [1] Bibring, Jean-Pierre, et al (2006) *science* 312(5772), 400-404. [2] Carter, J., et al. (2013) *Journal of Geophysical Research: Planets* 118(4), 831-858. [3] Bridges, John C., et al. (2001) *Space Science Reviews* 96(1), 365-392. [4] 4. Hicks, Leon J et al. (2014) *Geochimica et Cosmochimica Acta* 136, 194-210. [5] Treiman, Allan H. et al. (1993) *Meteoritics* 28(1), 86-97. [6] Bridges, J. C., and M. M. Grady. (2000) *Earth and Planetary Science Letters* 176(3-4), 267-279. [7] Baker, Ian, and Stephen E. Haggerty. (1967) *Contributions to Mineralogy and Petrology* 16(3), 258-273.

CARBON ISOTOPIC VARIATIONS OF GRAPHITES AND GRAPHITE-METAL INTERFACE IN KENDALL COUNTY IAB IRON METEORITE

Sourajit Sahoo*[1], Kuljeet Kaur Marhas[1], Vikram Goyal[1]

[1]Planetary Science Department, Physical Research Laboratory, Ahmedabad-380009, India
*Correspondence email.id: sourajit.sahoo@students.iiserpune.ac.in

The mechanism of formation of IAB iron meteorites is still unclear, and many hypotheses have been put forward to explain their unique trace elemental and morphological trends. [1-3], It has been proposed that IAB body with a size of >60km accreted within 1.4 Mya of CAI's but were later impact disrupted around 10-14Mya, leading to partial differentiated body, with metal pools [4]. Hf-W ages after GCR correction suggest that, the IAB-MG parent body accreted about 3-5 Mya [5], which is old for widespread melting by ^{26}Al or ^{60}Fe short-lived radioisotope systematics. Thus, impact-induced melting becomes the dominant process behind IAB iron meteorite formation. Our data conforms to the presence of primitive δ^{13}C in multiple phases in the meteorite and intra-grain δ^{13}C gradient in graphite crystallised within the metal matrix. The analysis was carried out on the Kendall County IAB iron meteorite sample mapped under SEM and analysed for δ^{13}C with the Cameca nano-SIMS 50 at Physical Research Laboratory, Ahmedabad.

Graphite modally occurs as linear crystals, forming a mesh of poorly interconnected network of parallel grains of sizes as small as 40x10 μm, or larger isolated elongated grains of upto 200 μm. While these morphologies are confined to Fe-Ni alloy zones (Kamacite/Taenite), in schreibersite (Fe_3P) or troilite (FeS), graphite occurs as spherulitic grains with diameters of 20μm or even smaller. We analysed carbon isotopic values of graphite embedded inside kamacite, troilite, schreibersite and also of the corresponding metal matrix surrounding the graphites(all data reported w.r.t Vienna Pee Dee Belemnite 13C universal reference). Graphite δ^{13}C values at the edges of the grains have a mean of -8.9‰, while core regions of graphites have a value of -12 ‰. The edges tend slightly towards a heavier δ^{13}C due to influx of more 13C compared to the slower diffusing 12C, and the matrix becomes progressively 13C rich as the graphite grows. The high degree of variability seen in our study is a signature of unequilibrated crystallisation and is a strong function of diffusivity and temperature. The interstitial self-diffusivity of carbon in kamacite is about 10^{-11}m^2/sec [7] at 1200K which is about the temperature at which these graphites were forming (1423-900 K) [8] and which is very fast compared to other trace elements. These δ^{13}C variations are thus, temperature influenced. The mean δ^{13}C of both troilitic graphite (-15.9‰) and schreibersitic graphite (-18.8‰) are lighter than the Fe-Ni graphite weighted mean (-7.2‰).

Carbon isotopic heterogeneity in iron meteorite graphite has been previously reported by [11] as having been influenced by interstellar heavy δ^{13}C graphite. Our work tries to explain this heterogeneity using petrology and computations based on prevailing physical conditions in the inner solar system. Following a top-down approach, a rapid cooling Fe-Ni reservoir, similar to cooling in impact mixing scenarios was modelled using a series of modified diffusion equation on ^{12}C,^{13}C species and compared with the experimental data. Ab-initio calculation and results obtained show that the graphite in kamacite is relatively light compared to the metal fractions. We hypothesize that δ^{13}C variation in intra and inter graphite is a sign of out-of-equilibrium formation of phases, in a chaotic environment (impact melting and remixing), which has cooled too rapidly to be able to homogenise with the metal surrounding the graphite.

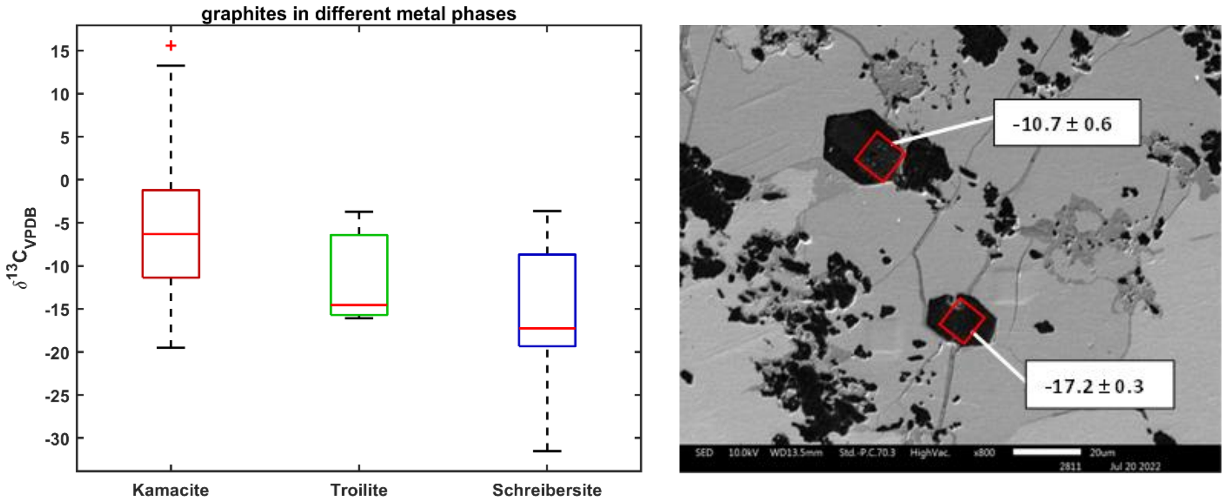

Figure 1-(a) Box and Whisker plot of $\delta^{13}C$ in different metal phases of kamacite, Troilite, Schreibersite. (b) Secondary electron SEM image showing $\delta^{13}C$ values of 2 hexagonal graphite(black) inside a Schreibersite host (dark grey), with kamacite sections in bottom left and right (light grey).

References- [1] Choi Byeon-Gak (1995)., GCA 59(3), 593-612.22 [2] Takeda, Hiroshi., (2000) GCA 64.7: 1311-1327. [3] Kracher, A.,(1985) J. Geophys. Res. 90(suppl.), C689-C698. [4] Hunt. C. Alison., Earth Planet. Sci. Lett., 312 (2011), pp. 390-400. [5] Worsham, E. A., (2017). Earth Planet. Sci. Lett, 467, 157{166}.[6] Buchwald., (1975) Handbook of Iron Meteorites. UC-Press, Berkeley, CA. [7] Mehrer, H. (2007). (Vol. 155). Springer Science & Business Media. [8] Massalski, T. B., (1986). Binary alloy phase diagrams (Vol. 1, No. 2). OH: ASM.[9] Kruijer, T., & Kleine, T. (2019)., GCA, 262, 92–103. [10] Marty (2013)., Rev Mineral Geochem 75:149–181. [11] Goresy,A. E.,(1995).,Nature, 373(6514), 496-499.

The Diyodar meteorite: A new fall in India

Y. Srivastava[1], A. Kumar[1], A. Basu Sarbadhikari[1,*], D. Ray[1], V. M. Nair[1], A. Das[1], A. D. Shukla[1], S. Sathiyaseelan[1], R. Ramachandran[1], B. Sivaraman[1], S. Vijayan[1], N. Panwar[1], A. J. Verma[1], N. Srivastava[1], A. Rani[1], G. Arora[1], R. R. Mahajan[1], And A. Bhardwaj[1]
[1]Physical Research Laboratory, Ahmedabad 380009, India
*Corresponding author E-mail: amitbs@prl.res.in

A meteorite fall is witnessed by the local villagers of Rantila and Ravel of Diyodar Taluka, Banaskantha district, Gujarat, India at around 19:30 hours (IST) on August 17, 2022. The meteorite fall has been observed in two nearby villages Rantila and Ravel ~10 km apart. During the fall, a large piece of the meteorite hit a neem tree branch and itself broke apart into several fragments due to the impact. The fragment has damaged the tiles floor of the porch of a household producing a small (~14 cm diameter and ~4-5 cm deep) crater. Several fragments of the meteorite were found scattered on the field around. The mass of the largest piece is around ~ 200 g and ~ 12 cm x 06 cm x 04 cm in size.

A group of PRL scientists visited the fall areas and collected two big fragments (~200 g and ~20 g) from the Tehsildar office at Diyodar. After interviewing several eyewitnesses and plotting the fall locations on the map, the trajectory of the meteorite is predicted from the southwest to a northeast direction. The meteorite fragments are fragile, and the inner materials are brittle. A light brown fusion crust (apparent thickness ~0.5 mm) is partly preserved over small areas in both the fragments, which indicates that the fragments are part of a bigger meteorite chunk. The sample is a stony achondrite breccia with a predominant constituent of white pyroxene grains of various size and shape. Large pyroxene grains (up to 2.0 cm) occur as bright white translucent crystals with two perfect sets of prismatic cleavages. The pyroxenes appear to be predominantly enstatitic in hand specimen.

Results from reflectance spectroscopy obtained at the Planetary Remote Sensing Laboratory, PRL revealed that the bulk meteorite sample indicates presence of two shallow absorption bands with band centers ~900 nm and ~1900 nm, which is typical of Mg-rich pyroxene enstatite.

The BSE imaging and mineral chemical analysis was carried out using Cameca SX 100 electron probe microanalyser (EPMA) at PRL. The modal abundance indicates the dominant mineral phase (~ 90 %) is enstatitic pyroxene (average value: Mg# 99.7, $En_{98.4}Wo_{1.0}$), while diopsidic pyroxene (average value: Mg# 99.8, $En_{54.5}Wo_{45.1}$) is also present as the next dominant phase (~ 5 %). Since the similar Mg-rich pyroxene occurs dominantly, the sample is a monomict breccia. Olivine is forsteritic (average value: Mg# 99.7), and plagioclase is albitic (average value: $Or_{3.3}Ab_{95.9}$). The mounted grains contain various sulfides.

Our preliminary description and study suggest that the meteorite is a rare, unique specimen of Aubrite (enstatite achondrite) [1], [2]. Indian subcontinent witnessed an exceptional record of meteorite falls (> 450 numbers of reported stony meteorite falls till date). However, this is the second reported aubrite fall in India, after Bustee fall in 1852 at Gorakhpur, Uttar Pradesh. Aubrites are the rare achondrite group of meteorites that originated from an extremely reduced differentiated parent body in our solar system [3], [4].

References: [1] Keil K. and Fredriksson K. (1963) *GCA,* **27**, 939-947. [2] Mittlefehldt D. W. et al. (1998) *Reviews in Mineralogy, Planetary Materials*, **36**, 4-1–4-195. [3] Krot A. N. et al. (2004). *Treatise on Geochemistry, Meteorites, Comets and Planets*, **1**, 83–128. [4] Barrat J. A. et al. (2016) *GCA,* **192**, 29-48.